Experimental Measurements and Modeling of a Helicon Plasma Source with Large Axial Density Gradients*

S.M. Tysk, C.M. Denning, J.E. Scharer, B.O. White, and M.K. Akhtar

Department of Electrical and Computer Engineering
University of Wisconsin – Madison 53706

Abstract. An investigation of wave magnetic field, density and temperature profiles, electron distribution function and wave-correlated Argon optical emission in a helicon plasma source is carried out. Diagnostics include Langmuir and wave magnetic field probes, interferometer, monochromator, and retarding field energy analyzer. The UW helicon experimental facility operates with argon pressures in the range of 1-300 mTorr. A variable capacitor matching network is used to couple up to 1.3 kW of pulsed RF power to a half-turn double-helix antenna. A uniform axial magnetic field of 200-1000 G is applied. Densities in the range of 10^{11}-$3x10^{13}$ cm^{-3} are obtained. Wave-correlated optical emission and modulation is externally measured at 443 nm corresponding to an upper state 35 eV above the neutral ground state and phase correlated with the 13.56 MHz antenna current. MAXEB, AntenaII, and nonlinear ionization codes are used to model the conditions present in the system and to provide a comprehensive picture of wave field behavior and fast and thermal electron ionization processes in a helicon source with strong axial density gradients.

INTRODUCTION

Helicon plasma sources are high efficiency, high density sources that operate over a wide range of densities (10^{11}-10^{13} cm^{-3}). Helicons are typically cylindrically symmetric with an axial magnetic field and operate at a radio frequency well above the ion cyclotron frequency. These sources have a wide range of applications including argon lasers[1], materials processing, and space based thruster systems[2].

An important question for helicon sources is the cause of the highly efficient ionization. The role of a non-Maxwellian fast electron component of the electron distribution function[3] in the helicon ionization process is currently an important issue. The existence of such a population of fast electrons is investigated using an optical diagnostic similar to that used by Ellingboe *et al.*[4] and Scharer *et al.*[5] on the WOMBAT helicon experimental facility. An important difference in this research is that the optical probe is located outside the Pyrex plasma chamber so that the plasma perturbations of the probe are negligible. Optical space-time measurements of the Ar II line emitted from a state 35 eV above the neutral ground state at 443 nm are made. Emission at 443 nm is indicative of the presence of a population of fast electrons which are required to populate the Ar II state through electron collisions.

CP694, *Radio Frequency Power in Plasmas: 15th Topical Conference on Radio Frequency Power in Plasmas,* edited by Cary B. Forest

Experimental Facility

A schematic of the radio-frequency helicon plasma source utilized for these experiments is shown in Figure 1. The plasma chamber is a 10 cm diameter Pyrex tube. The plasma chamber is pumped to a base pressure of $<10^{-6}$ Torr and 3 mT of argon is flowed through the antenna and chamber whereas the gas feed on WOMBAT is downstream. RF Power in the range of 600-800 W is coupled to the plasma with a half-turn double-helix antenna (dominant m = +1 mode) via a capacitive matching network. Less than 0.75 % of the RF power is reflected over the entire operating range. A set of 5 electromagnets is used to create a uniform axial magnetic field of 200-1000 Gauss. External optical probe and internal Langmuir, B-dot, and energy analyzer diagnostics are utilized. Internal diagnostics are retractable dog-leg systems capable of axial and radial scans that minimize plasma perturbations. Data is acquired using oscilloscopes and a GPIB interface and analyzed with Labview programs.

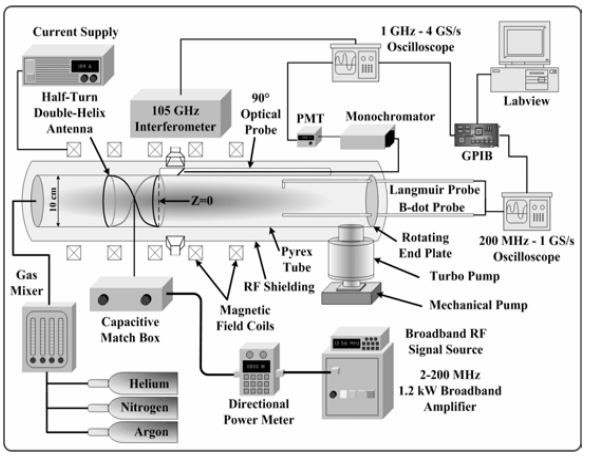

Figure 1: Schematic of UW Helicon Facility

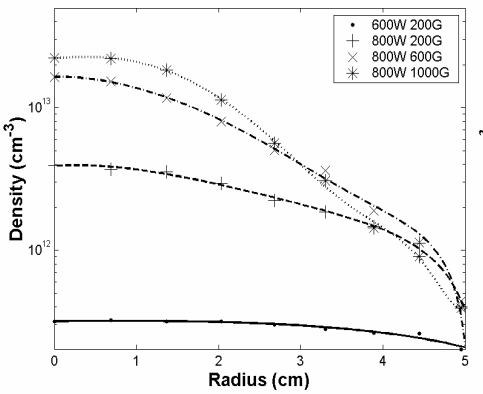

Figure 2: Radial Density Profiles (Z=15 cm)

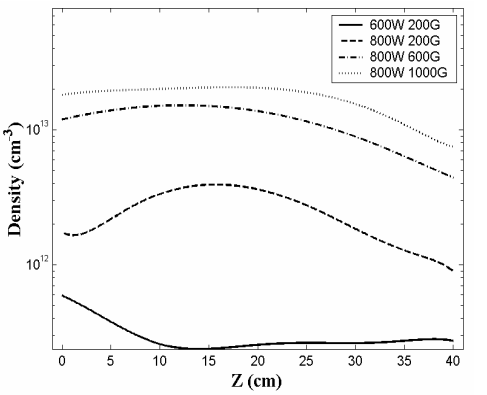

Figure 3: Axial Density Profiles (r=0 cm)

There are three distinct modes of operation for the aforementioned range of powers and axial (B_0) fields. The low density inductive mode exists at low power and low B_0 (<700W, <200G). The moderate density transition mode exists at lower power and lower B_0 (~700-800W, <400G). The high density helicon "blue" mode exists at higher power and higher B_0 (>800W, > 400G). These modes can be characterized by their axial and radial density profiles as shown in Figures 2 and 3. The inductive mode has a relatively uniform radial profile and an axial profile that peaks at the antenna and decays away. The transition mode has a broad radial profile and a highly downstream peaked axial profile. The helicon "blue" mode has a highly centrally peaked radial profile and moderate downstream peaked axial profile. Optical emission at 443 nm does not occur in the inductive mode begins in the transition mode and increases as power and magnetic field is increased.

Experimental Results

In this experiment the RF power delivered to the plasma is pulsed with a 10% duty cycle and a 6 ms pulse length. In the transition mode (800W, 200G) an initial high density transient (6×10^{12} cm^{-3}) occurs for the first 0.5 ms of the pulse and levels out for the following 2.0 ms (4×10^{12} cm^{-3}) and drops to a lower density (2×10^{12} cm^{-3}) for the final 3.5 ms of the pulse. Binning measurements are taken at 1.5 ms into the pulse with a 6 μs window that spans 85 RF periods. In the transition mode a traveling emission peak is observed as shown in Figure 4. The peak bin travels with a resonant electron phase velocity ($v_{\varphi 443} = \omega(\Delta z/\Delta\varphi)$) 2.4×10^{6} m/s corresponding to a resonant energy of 16.4 eV. Figure 4b shows the modulation depth for the transition mode increasing away from the antenna. This is indicative of an increasing contribution to the emission from wave correlated excitation. The modulated emission present in the helicon "blue" mode is close to the random level and would be the result of emission from "thermal" random background collisions. The dotted line in Figure 4b represents the measured average noise modulation resulting from a random signal input into the optical binning diagnostic.

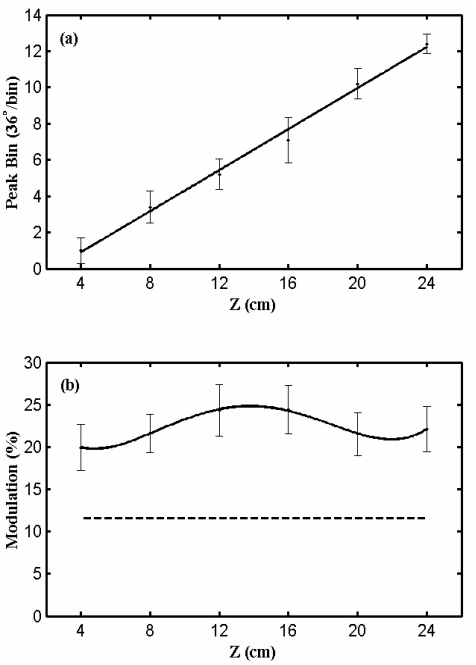

Figure 4: Transition Mode (800W, 200G) (a) Wave Correlated Emission (b) Modulation

The B_z wave magnetic field is measured with a small Pyrex enclosed five-

turn loop B-dot probe. The electrostatic signal is rejected using a hybrid combiner with a common mode rejection ratio of 38 dB. The AntenaII code is then used to model the E_z field in accordance with lab data using an axial averaged density. Figure 5 plots the wave phase velocity from the B-dot probe lab data and from the result of the AntenaII run along with the resonant electron phase velocity from the optical binning experiment. The phase velocity for all three cases show good agreement with an average phase velocity of 2.5×10^6 m/s corresponding to an average resonant electron energy of 18 eV. The wave phase velocity increases after this point and the emission drops off to a negligible value after z = 25 cm.

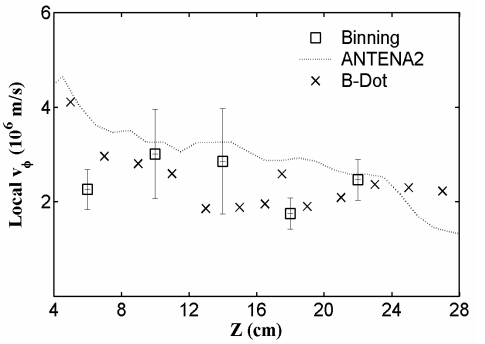

Figure 5: Transition Mode (800W, 200G) Phase Velocity Comparison

CONCLUSION

Ar II optical emission measured in the transition mode of the UW helicon experimental facility indicates a population of fast electron moving at the helicon wave phase velocity. Modeling results indicate a contribution to ionization of the argon case by non-Maxwellian components of the electron distribution function. This mode agrees well with the results of the WOMBAT experiment conducted at similar densities but at higher power and lower axial field magnetic field. The high density blue mode preliminary results indicate significantly reduced modulation indicating ionization primarily due to thermal processes. Energy analyzer data and further detailed modeling will describe the character of the helicon source in the transition and helicon "blue" modes.

ACKNOWLEDGEMENTS

*Research supported by NSF and in part by AFOSR.

REFERENCES

[1] P. Zhu and R. Boswell, Physics of Fluids B 3, 869 (1991)
[2] F. R. Chang Diaz, J. P. Squire, R. D. Bengston, B. N. Breizmann, F. W. Baity, and M. D. Carter, *Proc. of the 36th AIAA/ASME/SAE/ASEE Joint Propulsion Conference (Huntsville, AL 2000)*, No. 2000-3756
[3] A.W. Molvik, T.D. Rognlein, J.A. Byers, R.H. Cohen, A.R. Ellingboe, E.B. Hooper, H.S. McLean, B.W. Stallard, and P.A. Vitello, J. Vac. Sci. Techno. A 14 (3), 984 (1996).
[4] A. Ellingboe, R. Boswell, J. Booth, and N. Sadeghi, Physics of Plasmas 2 (6), 1807 (1995)
[5] J. Scharer, A. Degeling, G. Borg, and R. Boswell, Physics of Plasmas 9 (9), 3734 (2002).